

---

# DRIVING TOWARDS STABILITY AND EFFICIENCY: A VARIABLE TIME GAP STRATEGY FOR ADAPTIVE CRUISE CONTROL

---

**Shaimaa K. El-Baklish**

Institute for Transport Planning and Systems  
Department of Civil, Environmental and Geomatic Engineering  
ETH Zurich  
Zurich, Switzerland  
selbaklish@ethz.ch

**Anastasios Kouvelas**

Institute for Transport Planning and Systems  
Department of Civil, Environmental and Geomatic Engineering  
ETH Zurich  
Zurich, Switzerland  
kouvelas@ethz.ch

**Michail A. Makridis**

Institute for Transport Planning and Systems  
Department of Civil, Environmental and Geomatic Engineering  
ETH Zurich  
Zurich, Switzerland  
mmakridis@ethz.ch

## ABSTRACT

Automated vehicle technologies offer a promising avenue for enhancing traffic efficiency, safety, and energy consumption. Among these, Adaptive Cruise Control (ACC) systems stand out as a prevalent form of automation on today's roads, with their time gap settings holding paramount importance. While decreasing the average time headway tends to enhance traffic capacity, it simultaneously raises concerns regarding safety and string stability. This study introduces a novel variable time gap feedback control policy aimed at striking a balance between maintaining a minimum time gap setting under equilibrium car-following conditions, thereby improving traffic capacity, while ensuring string stability to mitigate disturbances away from the equilibrium flow. Leveraging nonlinear  $\mathcal{H}_\infty$  control technique, the strategy employs a variable time gap component as the manipulated control signal, complemented by a constant time gap component that predominates during car-following equilibrium. The effectiveness of the proposed scheme is evaluated against its constant time-gap counterpart calibrated using field platoon data from the OpenACC dataset. Through numerical and traffic simulations, our findings illustrate that the proposed algorithm effectively dampens perturbations within vehicle platoons, leading to a more efficient and safer mixed traffic flow.

**Keywords** Adaptive Cruise Control (ACC) · String Stability · Variable Time Gap · Nonlinear  $\mathcal{H}_\infty$  control

## 1 Introduction

Adaptive Cruise Control (ACC) is a part of the advanced driver assistance systems (ADAS) and is designed specifically for vehicle longitudinal control. In fact, ACC systems are the most widespread Society of Engineers (SAE) level 1 automated vehicle (AV) technology in the current markets [1]. For instance, 16 out of 20 best-selling cars in the US

market are equipped with an ACC system [2]. More importantly, vehicle automation gives rise to change traffic flow dynamics and to alleviate instabilities and congestion.

At its center, ACC employs a spacing policy which in turn determines the car-following behavior, platoon stability and traffic efficiency [3]. A small inter-vehicular spacing results in a higher traffic capacity but undermines safety and stability. The notion of stability referred to in this work is string stability. Intuitively, vehicles in a platoon are string stable if small perturbations from an equilibrium flow are dampened as they propagate in the upstream direction. Spacing policies in the literature can be categorized into 1) constant spacing (CS), 2) constant time-headway policies (CTH), and 3) variable time-headway (VTH) policies [4]. String stability was proved unattainable using CS policy without inter-vehicular communication to provide further information such as leader's acceleration [4, 5]. On the other hand, CTH and VTH policies can be appropriately designed to be string stable; nevertheless, there exists the conflicting objective of traffic efficiency. Using the OpenACC database for car-following experiments, the authors in [6] confirm that a string-stable ACC with large time-headway leads to poor road utilization decreasing capacity. In addition, a large headway threatens drivers' subjective acceptability due to possibly increased lane changes from adjacent lanes [3].

The aim of this work is to develop a VTH policy for ACC which is able to strike a balance between string stability and traffic efficiency. Under equilibrium flow, a CTH policy with a minimum time gap is adopted to promote efficient road utilization by ACC vehicles. This relies on the fact that stable driving conditions are most prevalent. This can also be supported by observed trajectory data from the OpenACC database. Figure 1 shows the distributions of instantaneous acceleration and deceleration which are mostly under  $\pm 0.5 \text{ m/s}^2$  for all platoons in the AstaZero and ZalaZone campaigns. However, perturbations/disturbances give rise to sharp acceleration/deceleration; raising safety, stability and efficiency concerns. Further investigations by Ciuffo et.al. compared short, medium and large time gap settings for field platoons in the ZalaZone experimental campaign in terms of traffic capacity [7]. They showed that short time gap platoons are able to attain the highest flow during stable conditions; while highly deteriorating during perturbations to relatively match medium time-gap platoons. Hence, the string instability is detrimental to the potential benefits of ACC systems to traffic flow. Therefore, the CTH policy must to be relaxed to allow for the needed larger gaps to attenuate such disturbances. To this end, a feedback  $\mathcal{H}_\infty$ -based VTH policy is adopted for guaranteed string stability. This scheme provides a compromise between enforcing traffic efficiency during equilibrium car-following conditions and attaining string stability during non-equilibrium flow by relaxation to the VTH policy.

## 2 Related Work

The most widely used ACC model is developed by [8] as a linear feedback control algorithm; where the acceleration is computed based on deviations away from a target speed (leading vehicle speed in car-following mode) and away from a target spacing determined by a constant time gap (CTG) policy. This spacing policy assumes that the space gap is proportional to the vehicle speed; thus, more appealing to drivers. Furthermore, Gunter et. al. have shown that commercially available ACC systems utilizing CTG policy are string unstable [9]. Interestingly, [2] presented simulations of string-unstable ACC vehicles platoon with a minimum time gap which enhanced downstream capacity relative to their string-stable counterpart with a maximum time gap. Lin et.al. demonstrated through experiments the need for different time gap setting in different driving scenarios in order to balance safety and driver's subjective acceptance [10].

Other variable spacing policies assume a nonlinear relationship between the space gap and the vehicle speed; thus, improving stability properties and traffic capacity. The authors in [11] proposed a nonlinear spacing policy as a function of speed and approaching rate; inspired by Greenshield's fundamental diagram (FD) and equations. The approaching rate is the relative speed of the ego vehicle to the leading vehicle. To enforce such a spacing policy, a sliding mode controller is implemented where the spacing is considered as the sliding variable. They have reported a 44% decrease in travel time compared to a CTG policy in simulations of a pipeline plus on-ramp network. Zhou and Peng have developed a quadratic spacing policy as a function of vehicle speed based on their investigation of human drivers' spacing policy [12]. They have designed the policy parameters to maximize the traffic capacity while imposing linear stability constraints. Again, a sliding mode controller is developed on top to implement the proposed spacing policy and the control scheme was tested in simulations of a merging scenario. Compared to a modified Greenshields-inspired spacing policy suggested by [13], the proposed scheme yielded a higher critical density and attenuated upstream perturbations in vehicles accelerations. All string stability analyses performed therein were in the strict sense and based on linear frequency-domain input-output  $\mathcal{H}_\infty$  gains. For more details on string stability analysis methods, the reader is referred to [14] and [15].

Variable time gap (VTG) policies can also be designed to achieve variable spacing. In [16], an intelligent driving strategy layer was suggested in order to regulate the ACC parameter settings according to the perceived traffic state. The authors aggregated traffic "situations" into five traffic states — free traffic, upstream jam front, congested traffic,

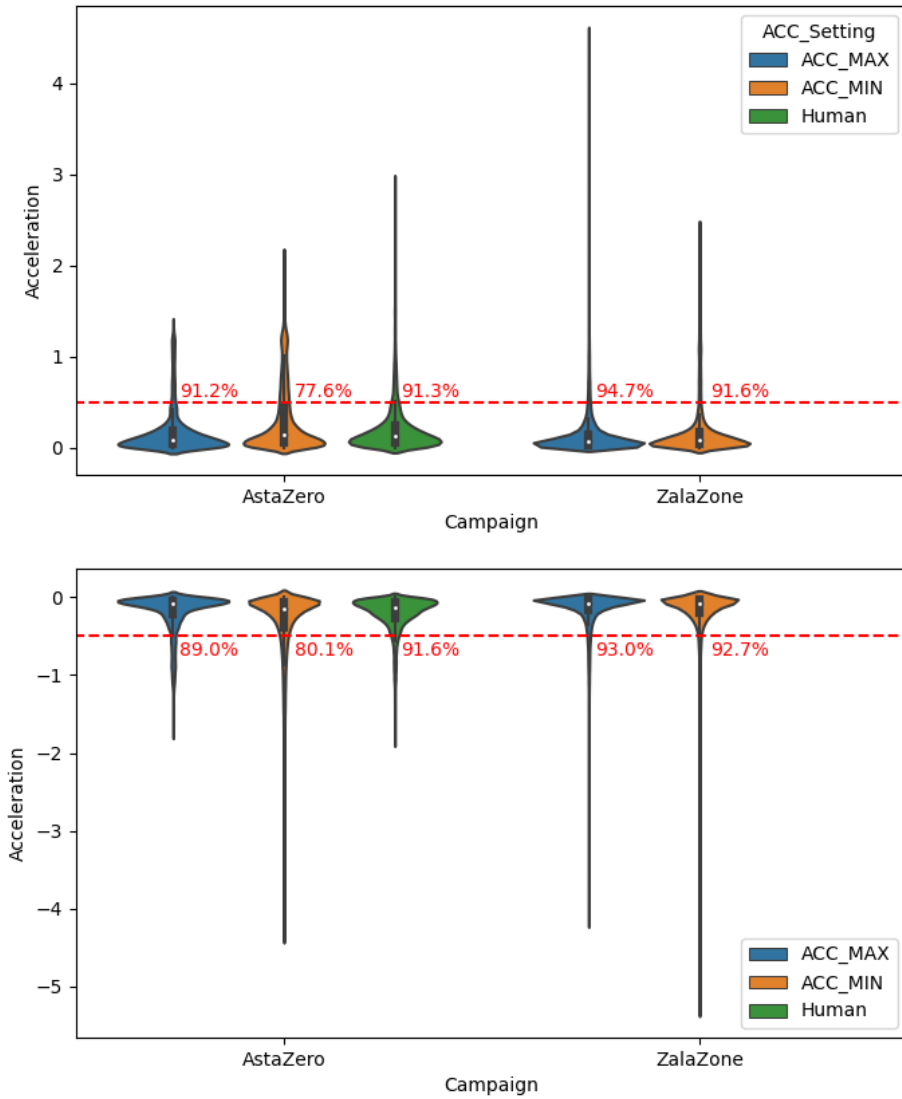


Figure 1: Distributions of instantaneous acceleration and deceleration of vehicles per campaign and driving mode. The red labels denote the cumulative proportion of acceleration/deceleration that is below/above  $\pm 0.5 \text{ m/s}^2$ .

downstream jam front, bottleneck sections — according to smoothed measurements of the space-mean speed and location information of active bottlenecks from the infrastructure. Then, a driving strategy matrix was developed to vary the ACC model parameters according to the perceived state. An Intelligent Driver Model (IDM) was used. For instance, the time gap was linearly decreased for the "downstream jam front" state. Simulations demonstrate a reduction in travel times for small penetration rates of 5%. Another VTG policy was proposed by [17]; where the time gap was varied linearly with the ratio between the measured space gap and the threshold space gap. The threshold space gap discriminates between cruising and car-following modes. The proposed VTG policy incentivizes shorter time gaps at larger space gaps that indicate higher densities. A two-regime model predictive control (MPC) scheme was implemented on top; where the costs represented safety and cruising and car-following modes efficiency. Spiliopoulou et. al. proposed adapting the time gap in real-time to the traffic flow state at a motorway section [18]. The applied time gap was the minimum of the desired setting of the driver and the suggested one that attempts to avoid congestion by increasing the static capacity of the section and, also increase the discharge flow at active bottleneck locations. Microscopic simulation for a motorway stretch with an on-ramp bottleneck show decrease in average vehicle delay and fuel consumption. These works showed improved traffic flow, but, without guarantees on string stability.

The work by [19] adapted the nonlinear spacing policies by [11, 20] based on macroscopic flow and [21] based on approaching rate. Hence, the developed ACC time gap strategy combined the vehicle speed, approaching rate, preceding vehicle acceleration, free-flow speed and jam density. Simulations using PTV-VISSIM of a single-lane highway with an on-ramp demonstrated diminished travel time and traffic delay compared to CTG policy and the VTG policy developed by [21]. A comparison between CTG and VTG policies for ACC was performed in [22]. The VTG policy employed varied with the approaching rate within the time gap bounds. The authors further investigated the linear stability and throughput of the mixed traffic flow. Both investigations and simulations have shown that a VTG policy is more likely to stabilize traffic flow and that an increased maximum time gap yields a more stable mixed traffic flow, but with a reduced capacity. A macroscopic approach towards designing the VTG policy was introduced in [23]. Bekiaris-Liberis and Delis assume the time gap of ACC vehicles as a control input to be manipulated to stabilize traffic flow expressed by an Aw-Rasclé-Zhang (ARZ) mixed traffic model. The feedback VTG control policy was developed for the linearized system around a uniform, congested equilibrium profile. Numerical simulations reported improved performance in terms of fuel consumption, travel time, and comfort compared to the CTG policy; which the authors proved to yield an unstable traffic flow.

In this work, we employ a VTG policy consisting of both a constant component; which may be a constant desired setting by the driver or a minimum time gap for efficient traffic flow, and a manipulated component to be designed in order to achieve string stability. This manipulated time gap component is developed as a feedback control policy; similar to [23], using nonlinear  $\mathcal{H}_\infty$  control in order to achieve  $\mathcal{L}_2$  string stability in the strict sense. A nonlinear analysis is necessary here due to the VTG strategy adopted. Also, formulation through strict string stability facilitates extending the platoon to any number of vehicles; since a platoon can be split to multiple leader-follower subsystems. Another important contribution presented here is a data-driven string stability analysis of vehicle platoons using empirical data collected from commercially available ACC-operated vehicles and manually driven vehicles. This approach is completely model-free and, hence, bypasses the need for calibration of car-following models to the experimental trajectory data to overcome any resulting biases.

### 3 Preliminaries

Consider a platoon of  $N + 1$  vehicles. The leader is denoted by the index 0. Each follower vehicle  $i, \forall i = 1, \dots, N$ , is described by the following state-space model.

$$\dot{s}_i(t) = v_{i-1}(t) - v_i(t) \quad (1a)$$

$$\dot{v}_i(t) = f_{a,i}(s_i(t), v_i(t), v_{i-1}(t)) \quad (1b)$$

where  $s_i$  and  $v_i$  denote the space headway and velocity of vehicle  $i$  respectively and  $v_{i-1}$  denotes the velocity of the preceding vehicle. The function  $f_{a,i}(\cdot)$  represents the longitudinal dynamics defined by car-following models such as the IDM [24] which may be homogeneous or heterogeneous.

A signal  $u(t) \in \mathcal{L}_2$  has, intuitively, bounded energy, i.e.  $\int_{t_0}^{\infty} u^T(t)u(t)dt < \infty$ , if it belongs to the Lebesgue space  $\mathcal{L}_2$  of square-integrable functions.

**Definition 1.** Let  $s_{eq,i}$  and  $v_{eq}$  be the equilibrium profile of (1),  $\mathbf{x}_i(t) = [s_i(t) - s_{eq,i} \quad v_i(t) - v_{eq,i}]^T$  be the deviation states away from the equilibrium profile and  $\delta v_{i-1}(t) = v_{i-1} - v_{eq}$ . For any platoon to be strictly input-to-state string-stable, follower vehicle  $i$  should have a local  $\mathcal{L}_2$ -gain equal to or less than  $\gamma, \gamma \leq 1$  for any initial state  $\mathbf{x}_i(0) \in \mathcal{N}$  if the response  $\mathbf{x}_i(t)$  to any disturbance from the preceding vehicle  $\delta v_{i-1}(t) \in \mathcal{L}_2[0, \infty)$  satisfies

$$\|\mathbf{x}_i(t)\|_{\mathcal{L}_2}^2 \leq \gamma^2 \left( \kappa(\mathbf{x}_i(0)) + \|\delta v_{i-1}(t)\|_{\mathcal{L}_2}^2 \right), \forall t \geq 0, i = 1, \dots, N \quad (2)$$

for some bounded function  $\kappa, \kappa(0) = 0$  and  $\mathcal{N} \subseteq \mathcal{X} \subseteq \mathbb{R}^2$  where  $\mathcal{X}$  is the set of admissible states.

**Definition 2.** Let  $\mathbf{X}_i(s)$  and  $\Delta V_{i-1}(s)$  be the Laplace transform of  $\mathbf{x}_i(t)$  and  $\delta v_{i-1}(t)$ . For a linear platoon to be strictly input-to-output string-stable, follower vehicle  $i$  should have an  $\mathcal{H}_\infty$ -norm or induced  $\mathcal{L}_2$ -gain equal to or less than  $\gamma, \gamma \leq 1$  if the response  $\mathbf{x}_i(t)$  to any disturbance from the preceding vehicle  $\delta v_{i-1}(t) \in \mathcal{L}_2[0, \infty)$  satisfies

$$\|\mathbf{\Gamma}_i(s)\|_{\mathcal{H}_\infty} = \sup_{\delta v_{i-1} \in \mathcal{L}_2(0, \infty) \neq 0} \frac{\|\mathbf{x}_i(t)\|_{\mathcal{L}_2}^2}{\|\delta v_{i-1}(t)\|_{\mathcal{L}_2}^2} \leq \gamma, \forall i = 1, \dots, N \quad (3)$$

where  $\mathbf{\Gamma}_i(s) = \frac{\mathbf{X}_i(s)}{\Delta V_{i-1}(s)}$  is the transfer function between follower vehicle  $i$  and its predecessor  $i - 1$ .

The  $\mathcal{L}_2$ -gain, or  $\mathcal{H}_\infty$ -norm for linear systems, represents the worst-case system gain over all excitations or input disturbances. Thus, if a platoon has an  $\mathcal{L}_2$ -gain of  $\gamma \leq 1$ , it means that perturbations will dissipate as they propagate upstream and the platoon will be string-stable.

For a platoon of ACC vehicles [8], the dynamic model can be written as follows.

$$\dot{s}_i(t) = v_{i-1}(t) - v_i(t) \quad (4a)$$

$$\dot{v}_i(t) = k_{1,i}(s_i(t) - s_0 - L_{i-1} - \tau_i v_i(t)) + k_{2,i}(v_{i-1}(t) - v_i(t)) \quad (4b)$$

where  $s_0$  is the standstill distance,  $L_{i-1}$  is the length of vehicle  $i - 1$  and  $k_{1,i}$ ,  $k_{2,i}$  and  $\tau_i$  are the spacing control gain, velocity control gain and the constant time gap for ACC vehicle  $i$ . The CTG spacing policy is defined as  $s_{\text{des},i} = s_0 + L_{i-1} + \tau_i v_i(t)$ .

To define the error dynamics of a leader-follower subsystem, the equilibrium profile is defined by the constant speed  $v_{\text{eq}}$  at which all vehicles are travelling at. The equilibrium space headway is given as  $s_{\text{eq},i} = s_0 + L_{i-1} + \tau_i v_{\text{eq}}$ . Then, the deviation states are expressed as  $\tilde{s}_i = s_i - s_{\text{eq},i}$  and  $\tilde{v} = v_i - v_{\text{eq}}$  and the deviation dynamics are derived as follows.

$$\dot{\tilde{s}}_i = v_{i-1} - v_i \quad (5a)$$

$$= (v_{i-1} - v_{\text{eq}}) - (v_i - v_{\text{eq}}) \quad (5b)$$

$$= -\tilde{v}_i + \delta v_{i-1} \quad (5c)$$

$$\dot{\tilde{v}}_i = k_{1,i}(s_i(t) - s_0 - L_{i-1} - \tau_i v_i(t)) + k_{2,i}(v_{i-1}(t) - v_i(t)) \quad (6a)$$

$$= k_{1,i}(s_i(t) - s_0 - L_{i-1} - \tau_i(\tilde{v}_i + v_{\text{eq}})) + k_{2,i}(-\tilde{v}_i + \delta v_{i-1}) \quad (6b)$$

$$= k_{1,i}(s_i(t) - s_0 - L_{i-1} - \tau_i v_{\text{eq}}) - k_{1,i}\tau_i \tilde{v}_i - k_{2,i}\tilde{v}_i + k_{2,i}\delta v_{i-1} \quad (6c)$$

$$= k_{1,i}\tilde{s}_i - k_{1,i}\tau_i \tilde{v}_i - k_{2,i}\tilde{v}_i + k_{2,i}\delta v_{i-1} \quad (6d)$$

where  $\delta v_{i-1}$  denotes the deviation of the leader's velocity away from the equilibrium velocity and represents a disturbance to the considered leader-follower subsystem.

## 4 Data-Driven String Stability Analysis of Adaptive Cruise Control

Due to propriety issues, the true model of ACC controllers is not known. Therefore, researchers proposed many models in the literature, most notably the one by [8], to analyze ACC controllers and their performance. However, retrieving a meaningful model which calibrates well to trajectory data from commercially available ACC systems is challenging requiring time and expert knowledge. Also, conclusions drawn from calibrated models may be subject to biases acquired from the optimization and calibration procedure. In this section, a direct data-driven approach for strict string stability analysis with the assumption of linear platoon model is performed using only trajectory data and bypassing the need for model calibration [25, 26].

### 4.1 Data-Driven $\mathcal{L}_2$ -gain Estimation

Consider a single-input single-output (SISO) linear time-invariant (LTI) system  $G(s)$ . In our case, the system input is the disturbing leader velocity  $\delta v_{i-1}(t)$  and the system output may be either the deviation of follower velocity  $\tilde{v}_i(t)$  or the deviation of space headway  $\tilde{s}_i(t)$ . Trajectory data of length  $N_D$  is assumed to be available. A matrix  $T_m(\delta v_{i-1}) \in \mathbb{R}^{(N_D+m-1) \times m}$  is formed of  $m$  columns of the downshifted input signal where  $m < N_D$ .

$$T_m(\delta v_{i-1}) = \begin{bmatrix} \delta v_{i-1}(1) & 0 & \dots \\ \delta v_{i-1}(2) & \delta v_{i-1}(1) & \dots \\ \vdots & \ddots & \ddots \\ \delta v_{i-1}(N_D) & \vdots & \ddots \\ 0 & \delta v_{i-1}(N_D) & \ddots \\ \vdots & 0 & \ddots \\ \vdots & \vdots & \ddots \end{bmatrix} \quad (7)$$

Then, the estimated auto-correlation matrix is defined as  $\hat{R}_m(\delta v_{i-1}) = \frac{1}{N_D} T_m^T(\delta v_{i-1}) T_m(\delta v_{i-1}) \in \mathbb{R}^{m \times m}$ . Each entry in this matrix represents estimates of the auto-correlation function  $\hat{R}_{uu}(T) = \frac{1}{N_D} \sum_{t=1}^{N_D-T} u(t)u(t+T)$ .

**Assumption 1.** A linear time-invariant (LTI) system is persistently excited if the auto-correlation matrix of the input  $u$  data trajectory of length  $N_D$  is full rank, i.e.  $\text{rank}(\hat{R}_m(u)) = \frac{1}{N_D} T_m^T(u) T_m(u) = m$ .

Similar matrices exist for the outputs as well. Provided that Assumption 1 is satisfied, we can define the following semi-definite program to estimate the  $\mathcal{H}_\infty$ -norm or  $\mathcal{L}_2$ -gain of the underlying system.

$$\hat{\gamma} = \min_{\gamma} \gamma \quad (8a)$$

$$\text{s.t. } \frac{1}{N_D} T_m^T(y) T_m(y) - \gamma^2 \frac{1}{N_D} T_m^T(\delta v_{i-1}) T_m(\delta v_{i-1}) \leq 0, \gamma \geq 0 \quad (8b)$$

where  $\hat{\gamma}$  is the estimated  $\mathcal{L}_2$ -gain and  $y$  denotes the selected system output which can be  $\tilde{v}_i(t)$  or  $\tilde{s}_i(t)$ . The estimated  $\mathcal{L}_2$ -gain converges to the true value, i.e.  $\hat{\gamma}^2 \rightarrow \|G(s)\|_{\mathcal{H}_\infty}^2$ , as trajectory data length becomes infinite  $N_D \rightarrow \infty$ ,  $m \rightarrow \infty$  and  $\frac{m}{N_D} \rightarrow 0$  [27]. This quantifies the system norm needed to make conclusions about strict string stability for linear platoons, as per Definition 2.

## 4.2 Field Data Description

The empirical data were taken from two experimental campaigns which took place in AstaZero and ZalaZone proving grounds in Sweden and Hungary respectively. The AstaZero campaign consisted of a fleet of 5 commercially available ACC-equipped vehicles on the 5.7-km-long Rural Road; while, a fleet of 10 vehicles was deployed on the circular Dynamic Platform (300-m diameter) in the ZalaZone campaign. Both campaigns were carried out in 2019.

In all campaigns, data acquisition was performed using high-accuracy on-board equipment (e.g. U-blox global navigation satellite system (GNSS) receivers) with a sampling frequency at 10 Hz. Maximum and minimum time gap settings were used for the ACC-operated tests in both campaigns. Also, some tests were carried out without ACC operation (i.e. manual driving) in the AstaZero campaign. These data can be freely accessed through the OpenACC database [6].

## 4.3 String Stability of Field Platoons

Each platoon was divided into leader-follower subsystems; where the convex program (8) was solved to estimate the  $\mathcal{L}_2$ -gain of the corresponding subsystem and, subsequently, provide numerical thresholds for strict string stability.

The speed-to-speed relation was examined; i.e. the output was taken to be the deviation in the follower velocity  $y(t) = \tilde{v}_i(t)$ . The equilibrium velocity  $v_{\text{eq}}$  was taken to be the median velocity of the leading vehicle for 1-minute intervals in the duration of the car-following maneuver.

Figure 2 illustrates the distribution of the estimated  $\mathcal{L}_2$ -gain values of all leader-follower subsystems according to the ACC settings ('MIN'/'MAX' for minimum/maximum time gap ACC setting and 'HUMAN' for manual driving). A maximum time gap ACC setting has consistently lower  $\mathcal{L}_2$ -gains; even for the same make and model of the tested vehicle. Audi, Jaguar and Tesla car-makes record the lowest  $\mathcal{L}_2$ -gain values, as observed from Figure 2. In addition, manual driving is shown to be string stable with 87.5% of the  $\mathcal{L}_2$ -gain estimates below the string stability threshold of  $\gamma = 1$ . This mainly due to the variable spacing policy adopted by human drivers.

As demonstrated in Figure 3, the first vehicles inside the platoon show higher  $\mathcal{L}_2$ -gain estimates which show that they are more susceptible to disturbances in the driving cycle from the platoon leader and, thus, have a crucial role in dissipating such disturbances. This case is more notable for the minimum time gap ACC setting.

The findings demonstrated in Figures 2 and 3 second those of [9] that commercially available ACC vehicles are string unstable. These findings are based on the assumption of linearity of the underlying system; hence, possible extensions to data-driven nonlinear analysis; specifically for variable spacing policies, are interesting for future research.

## 5 Synthesis of $\mathcal{H}_\infty$ -based Variable Time Gap Control Policy

In this section, a VTG control policy is designed to guarantee strict string stability during conditions away from the equilibrium profile,  $s_{\text{eq},i}$  and  $v_{\text{eq}}$ , of the ACC model in (4). Consider the following form of the time gap command

$$\tau_i = \tau_i^* + u_i(t) \quad (9)$$

where  $\tau_i^*$  and  $u_i(t)$  are the constant and variable time gap components respectively. The deviation dynamics for follower vehicle  $i$  can be then derived similar to (5) and (6) and are expressed as

$$\dot{\tilde{s}}_i(t) = \tilde{v}_i(t) + \delta v_{i-1}(t) \quad (10a)$$

$$\dot{\tilde{v}}_i(t) = k_{1,i} \tilde{s}_i(t) - (k_{1,i} \tau_i^* + k_{2,i}) \tilde{v}_i(t) + k_{2,i} \delta v_{i-1}(t) - k_{1,i} (v_{\text{eq}} + \tilde{v}_i(t)) u_i(t) \quad (10b)$$

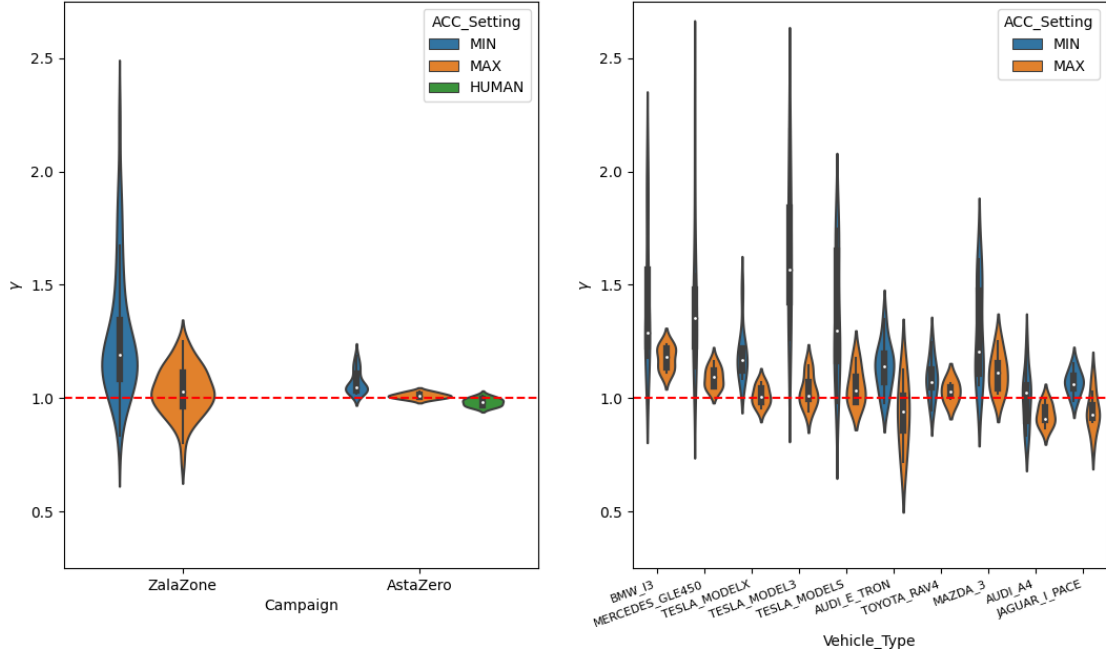


Figure 2: Distribution of estimated  $\mathcal{L}_2$ -gains for all leader-follower subsystems per campaign (left) and per vehicle make and model (right). The red dashed line represents the threshold of string stability at  $\gamma = 1$ .

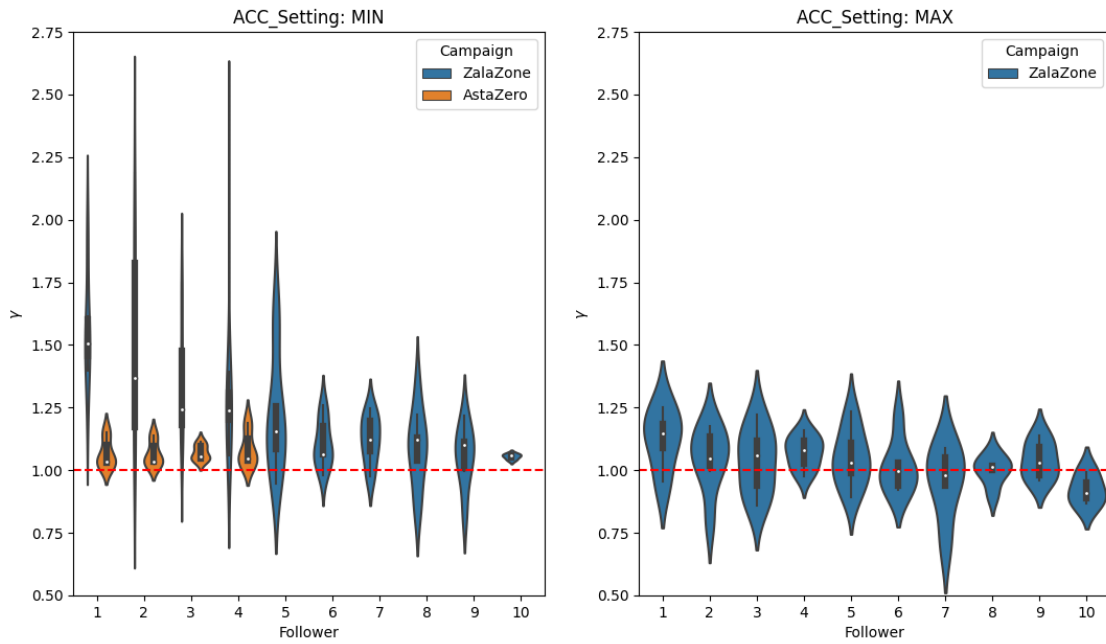


Figure 3: Distribution of estimated  $\mathcal{L}_2$ -gains for all leader-follower subsystems per vehicle order in platoon for minimum (left) and maximum (right) time gap ACC settings. The red dashed line represents the threshold of string stability at  $\gamma = 1$ .

where  $\delta v_{i-1}(t)$  is considered as the disturbance from the preceding vehicle to be attenuated by the control input  $u_i(t)$ . The system states are denoted by the vector  $\mathbf{x}_i(t) = [\tilde{s}_i(t) \quad \tilde{v}_i(t)]^T$ .

For strict input-to-state string stability, the VTG control policy for  $u_i(t)$  needs to be designed to yield an  $\mathcal{L}_2$ -gain of  $\gamma \leq 1$ . Notably, the system is nonlinear due to the last term in (10b). To this end, a synthesis of nonlinear  $\mathcal{H}_\infty$  controller ensues.

The nonlinear system is represented as in the following standard state-space form

$$\dot{\mathbf{x}} = f(\mathbf{x}) + g_1(\mathbf{x})\mathbf{w} + g_2(\mathbf{x})\mathbf{u} \quad (11a)$$

$$\mathbf{z} = h(\mathbf{x}) + K_{12}(\mathbf{x})\mathbf{u} \quad (11b)$$

where the subscript  $i$  is dropped for brevity,  $\mathbf{w} = \delta v_{i-1}$  denotes the exogenous disturbance,  $\mathbf{u} = u_i$  denotes the control input, and  $\mathbf{z} = [\rho_s \tilde{s}_i \quad \rho_v \tilde{v}_i \quad \rho_u u_i]$  denotes the penalty variables with penalty weights of  $\rho_s, \rho_v$  and  $\rho_u$ . Thus, the vector-valued functions are given as follows.

$$f(\mathbf{x}) = \begin{bmatrix} -\tilde{v}_i \\ k_{1,i} \tilde{s}_i - (k_{1,i} \tau_i^* + k_{2,i}) \tilde{v}_i \end{bmatrix} \quad (12a)$$

$$g_1(\mathbf{x}) = \begin{bmatrix} 1 \\ k_{2,i} \end{bmatrix} \quad (12b)$$

$$g_2(\mathbf{x}) = \begin{bmatrix} 0 \\ -k_{1,i}(v_{\text{eq}} + \tilde{v}_i) \end{bmatrix} \quad (12c)$$

$$h(\mathbf{x}) = [\rho_s \tilde{s}_i \quad \rho_v \tilde{v}_i \quad 0]^T \quad (12d)$$

$$K_{12}(\mathbf{x}) = [0 \quad 0 \quad \rho_u]^T \quad (12e)$$

$$h^T(\mathbf{x})K_{12}(\mathbf{x}) = 0, \quad K_{12}^T(\mathbf{x})K_{12}(\mathbf{x}) = R_2 = \rho_u^2 \quad (12f)$$

The problem of designing  $\mathbf{u}$  for string stability, as per Definition 1, can be formulated as an infinite-time horizon min-max optimization problem so that the  $\mathcal{L}_2$ -gain from  $\mathbf{w}$  to  $\mathbf{z}$  is  $\gamma \leq 1$ .

$$\mathbf{u}^* = \arg \min_{\mathbf{u} \in \mathcal{U}} \max_{\mathbf{w} \in \mathcal{L}_2} \frac{1}{2} \int_0^\infty \|\mathbf{z}(t)\|^2 - \gamma^2 \|\mathbf{w}(t)\|^2 dt \text{ subject to (11)} \quad (13)$$

where  $\mathcal{U} \subseteq \mathbb{R}$  is the set of admissible control inputs. Here, the objective function balances the minimization of the penalty variables, i.e. performance specifications, against the worst-case exogenous disturbances. Notably, the penalty variables  $\mathbf{z}(t)$  include the deviation of the space headway away from the equilibrium profile  $s_{\text{eq},i}$  and the manipulated time gap command  $u_i(t)$ . This motivates minimizing the space headway, as an incentive to more efficient road utilization and traffic capacity from a microscopic perspective, and the manipulated time gap command to maintain proximal operating conditions to the constant time gap setting  $\tau_i^*$ .

This optimization problem is also a differential game; consisting of a two-player zero-sum game. The minimizing player controls the input  $\mathbf{u}$ ; whereas the maximizing player controls the disturbance  $\mathbf{w}$ . This game has a saddle-point equilibrium solution if it has a value function  $V : \mathcal{X} \mapsto \mathbb{R}$  that is positive definite and satisfies the Hamilton-Jacobi-Isaacs (HJI) equation and the optimal feedback policies of both players [28]

$$\mathbf{u}^* = -R_2^{-1}(\mathbf{x})g_2^T(\mathbf{x})V_x \quad (14a)$$

$$\mathbf{w}^* = \frac{1}{\gamma^2}g_1^T(\mathbf{x})V_x \quad (14b)$$

$$V_x f(\mathbf{x}) + \frac{1}{2}h^T(\mathbf{x})h(\mathbf{x}) + \frac{1}{2}V_x \left( \frac{1}{\gamma^2}g_1(\mathbf{x})g_1^T(\mathbf{x}) - g_2(\mathbf{x})R_2^{-1}g_2^T(\mathbf{x}) \right) = 0 \quad (14c)$$

where  $V_x$  is the Jacobian matrix of  $V(\mathbf{x})$ . A closed form solution for (14c) does not exist, thus, a numerical approximation using Taylor's series is adopted. Then, the HJI equation becomes an algebraic Ricatti equation of the following

form to be solved online; since we consider the equilibrium velocity as the subsystem leader velocity  $v_{\text{eq}} = v_{i-1}$ .

$$PA + A^T P + P \left( \frac{1}{\gamma^2} B_1 B_1^T - B_2 R_2^{-1} B_2^T \right) P + C^T C = 0 \quad (15a)$$

$$f(\mathbf{x}_i) = A \mathbf{x}_i + \hat{f}^{[2+]}(\mathbf{x}_i); A = \begin{bmatrix} 0 & -1 \\ k_1 & -(k_1 T_g^* + k_2) \end{bmatrix} \quad (15b)$$

$$g_1(\mathbf{x}_i) = B_1 + \hat{g}_1^{[1+]}(\mathbf{x}_i); B_1 = \begin{bmatrix} 1 \\ k_2 \end{bmatrix} \quad (15c)$$

$$g_2(\mathbf{x}_i) = B_2 + \hat{g}_2^{[1+]}(\mathbf{x}_i); B_2 = \begin{bmatrix} 0 \\ -k_1 v_e \end{bmatrix} \quad (15d)$$

$$h(\mathbf{x}_i) = C \mathbf{x}_i + \hat{h}^{[2+]}(\mathbf{x}_i); C = \begin{bmatrix} \rho_s & 0 \\ 0 & \rho_v \\ 0 & 0 \end{bmatrix} \quad (15e)$$

$$V(\mathbf{x}_i) = \mathbf{x}_i^T P \mathbf{x}_i + \hat{V}^{[3+]}(\mathbf{x}_i) \quad (15f)$$

The  $n^{\text{th}}$ -order and higher-order terms of the function  $(\cdot)(\mathbf{x}_i)$  are denoted by  $(\cdot)^{[n+]}(\mathbf{x}_i)$  and  $P \succeq 0$  is a symmetric positive definite matrix. Note that, in our setting, the only assumptions made are (15d) and (15f) and the rest are exact expressions. On another note, the algebraic Ricatti equation in (15a) is feasible for a prescribed  $\gamma$  if the pair  $(A, B_2)$  is stabilizable and the Hamiltonian matrix

$$H = \begin{bmatrix} A & \left( \frac{1}{\gamma^2} B_1 B_1^T - B_2 R_2^{-1} B_2^T \right) \\ -C^T C & -A^T \end{bmatrix}$$

is dichotomic, i.e. has no eigenvalues on the imaginary axis. This is true for  $v_{\text{eq}} > 0$  and for an appropriate choice of penalty weights,  $\rho_s$ ,  $\rho_v$  and  $\rho_u$ . The VTG control strategy can be illustrated in Figure 4.

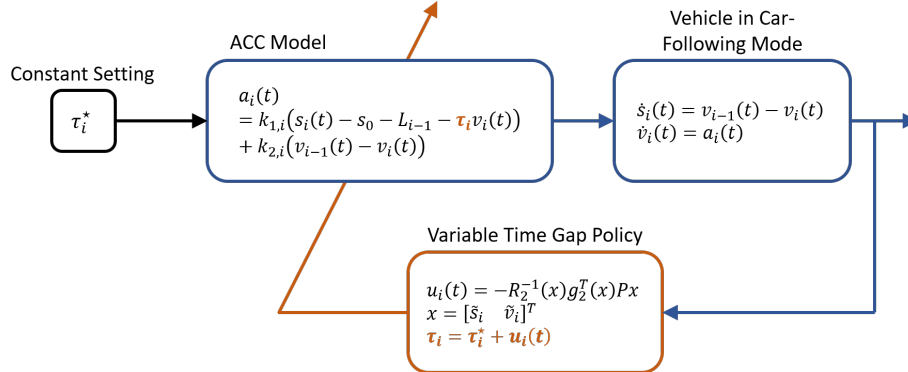


Figure 4: Block diagram of the VTG proposed feedback control policy.

This VTG policy is robust to velocity disturbances from the leader away from the equilibrium profile; thus it yields a string-stable system in the strict sense with a worst case  $\mathcal{L}_2$ -gain of  $\gamma \leq 1$ . It also guarantees the internal stability of the considered vehicle  $i$ . Additionally, the constant time gap setting can be kept either at minimum setting for benefits in traffic efficiency or at a desired setting chosen by the driver. Hence, the time gap parameter design is modularized by separating string stability from other considerations.

## 6 Numerical Simulations

In this section, the performance of the proposed VTG ACC scheme will be investigated against the CTG ACC scheme [8] calibrated in field platoon data. The numerical simulations are performed on real driving cycles from the OpenACC dataset to demonstrate the efficacy of the proposed VTG ACC scheme versus commercially available ACC systems. An implementation is openly available at <https://github.com/shaimaa-elbaklish/vtg-acc>.

## 6.1 Performance Indices

In order to assess the performance of the different ACC algorithms, several indices are introduced to quantify the achieved performance. The first performance indicator is used to measure the propagation of perturbations upstream and estimate the  $\mathcal{L}_2$ -gain,  $\gamma$ , of the predecessor-follower subsystems at worst-case scenario. It can be estimated from simulated trajectories using the approach presented in Section 4. The estimated  $\hat{\gamma}$  computed via the semi-definite program in (8) represents the string stability aspect.

Furthermore, Time-To-Collision (TTC) is used as a safety surrogate measure and is defined instantaneously as

$$TTC_i(t) = \frac{s_i(t)}{v_i(t) - v_{i-1}(t)} \quad (16)$$

which is valid in car-following situations where the following vehicle is faster than the preceding one,  $v_i(t) > v_{i-1}(t)$ . The last indicator is used to quantify the energy efficiency aspect and is the tractive energy consumption of a vehicle [29].

$$P_i = \max \left( 0, 10^{-3} v_i (F_0 + F_1 v_i + F_2 V_i^2 + 1.03 m a_i + m g \sin \theta) \right) \quad (17a)$$

$$E_i = \frac{\int_0^T P_i dt}{0.036 \int_0^T v_i dt} \quad (17b)$$

Tractive energy consumption takes into account only tractive power demand so that it is agnostic to vehicle specifications; enabling a fair comparison between different ACC algorithms. The road is assumed horizontal;  $\theta = 0$ . The road-related coefficients  $F_0 = 213$  N,  $F_1 = 0.0861$  Ns/m,  $F_2 = 0.0027$  Ns<sup>2</sup>/m<sup>2</sup> and the vehicle's mass  $m = 1500$  kg are assumed constant over all vehicles in order to normalize over the different platoons and compare the performance of the utilized ACC algorithms.

## 6.2 Driving Cycles from Field Data

In order to assess the performance of the proposed VTG ACC scheme, real driving cycles are used from the AstaZero campaign available in the OpenACC dataset [6]. The field platoon data used here is acquired using minimum setting for the ACC systems of all vehicles in the platoon. First, the CTG ACC model by [8] is calibrated against each leader-follower subsystem's data trajectories. The calibration process is carried out through the following optimization program [30]

$$\beta^* = \arg \min_{\beta} \gamma_a f_{\text{NRMSE}}(a_i) + \gamma_v f_{\text{NRMSE}}(v_i) + \gamma_s f_{\text{NRMSE}}(s_i) \quad (18a)$$

$$\text{subject to } \beta \in \Omega_{\beta} \quad (18b)$$

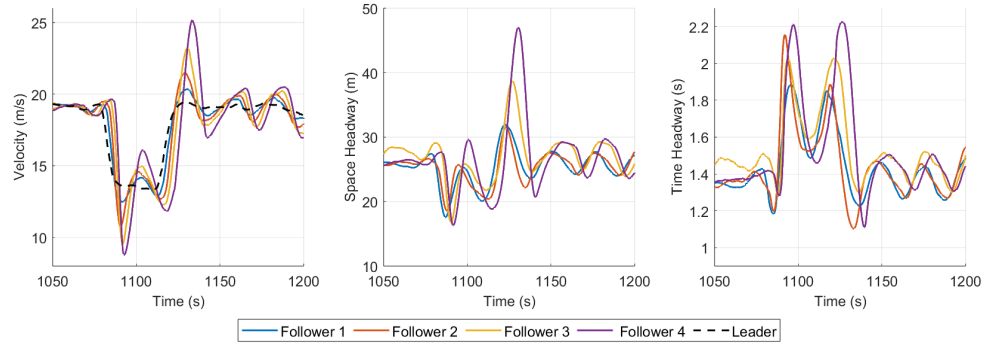
$$\beta = [k_{1,i} \quad k_{2,i} \quad \tau_i]^T \quad (18c)$$

$$f_{\text{NRMSE}}(y) = \frac{\sqrt{\frac{1}{T} \sum_{t=0}^T (y_{\text{sim}}(t) - y_{\text{obs}}(t))^2}}{\sqrt{\frac{1}{T} \sum_{t=0}^T y_{\text{obs}}^2(t)}} \quad (18d)$$

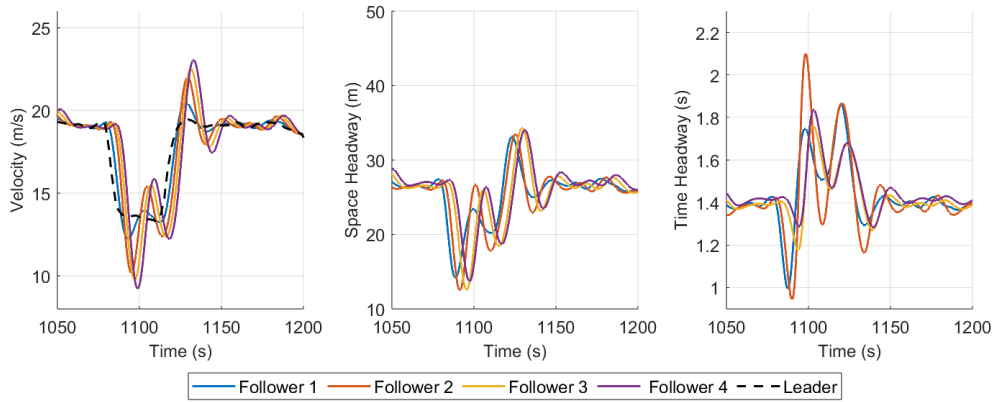
where  $f_{\text{NRMSE}}(y)$  is the normalized root mean squared error function used as a goodness of fit measure for the signal  $y$  and  $\Omega_{\beta}$  is the set of admissible parameters  $\beta$ . The simulated and observed (i.e. from data) trajectories of the signal  $y$  are denoted by  $y_{\text{sim}}(t)$  and  $y_{\text{obs}}(t)$  respectively. The same parameter values for the calibrated CTG ACC model are used for the proposed scheme; i.e.  $k_{1,i}$ ,  $k_{2,i}$  and  $\tau_i^*$ .

Figure 5 shows an excerpt of the trajectories of the first and last following vehicles in the platoon. The perturbations in leader velocity are magnified in the upstream direction. While, the VTG ACC scheme exhibits a robust and resilient performance against these disturbances. Also, the proposed algorithm records significant reduction in space and time headways with respect to the calibrated CTG ACC and the data collected from commercially available ACC systems. Also, it is noteworthy that the proposed scheme adheres to the selected constant time headway policy  $\tau_i^*$  during stable car-following conditions and deviates away from it to attenuate any disturbances as intended.

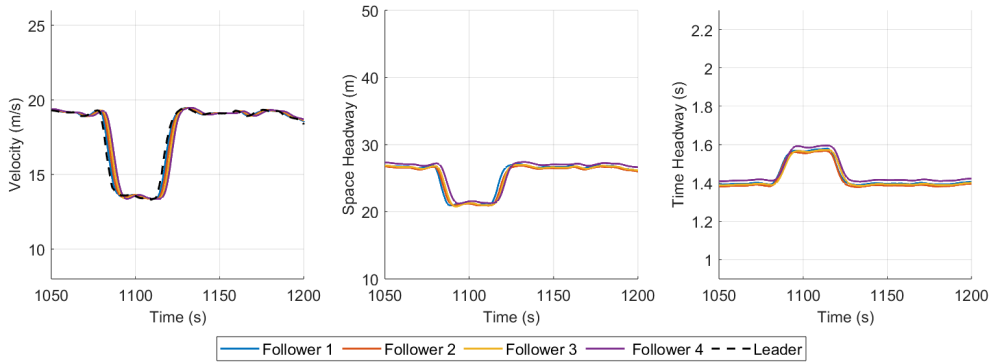
The performance indicators for each following vehicle in the aforementioned experiment are illustrated in Figure 6. The estimated  $\mathcal{L}_2$ -gains for VTG ACC are the lowest compared to the calibrated CTG ACC model and those estimated from field data; indicating better string stability. However, it should be mentioned that the estimation approach in (8) is under the assumption of LTI systems; whereas, the VTG ACC algorithm is nonlinear. Therefore, the computed gains may be overestimated. The proposed VTG ACC algorithm achieves higher performance in terms of safety and tractive



(a) OpenACC Data



(b) Calibrated CTG ACC



(c) Proposed VTG ACC

Figure 5: Simulated trajectories of a platoon of 5 vehicles along a straight road using the calibrated CTG ACC and the proposed VTG ACC. Platoon leader velocity is the black dashed line from AstaZero experimental campaign. All vehicles in this platoon are using ACC with minimum time gap settings.

energy consumption; where the energy consumption is conformed along the entire platoon and higher TTC values are achieved. This difference is quite pronounced for the first follower since it is the immediate following vehicle to the perturbing one (i.e. platoon leader) as the proposed scheme relaxes its time gap policy to attenuate perturbations. In addition, the CTG ACC shows higher energy consumption overall the platoon members due to the disturbances propagation along the platoon. Hence, safety and energy efficiency concerns raised due to string instability are relieved using the proposed approach while optimizing road space utilization by adhering to a minimum time gap during stable car-following conditions.

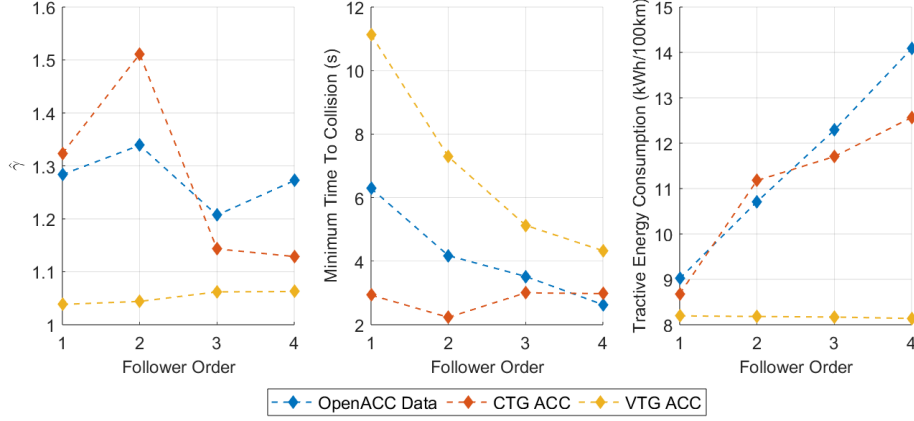


Figure 6: Performance indicators for a platoon of 5 vehicles along a straight road using the calibrated CTG ACC and the proposed VTG ACC.

## 7 Traffic Simulations

In this section, an investigation of the proposed scheme is carried out from a traffic flow perspective to validate our findings and the potential benefits of the proposed algorithm. Simulation of Urban Mobility (SUMO) is used for microscopic simulations. The proposed algorithm (VTG ACC) will be tested against the CTG ACC [8], two string-stable controllers from the literature [12, 31], and the IDM models. Again, field platoon data from OpenACC dataset were used to calibrate the CTG ACC model for commercially available ACC-equipped vehicle with minimum time gap settings. The same calibrated parameters are used for the VTG ACC as well. Also, manual driving data from AstaZero campaign in the OpenACC dataset is utilized for calibration of IDM to model human driving; which will be termed "IDM Human" in the subsequent sections.

The approach adopted by [12] utilizes a quadratic spacing policy inspired from human driving behavior and optimized for string stability and maximum traffic capacity. The desired space headway  $s_{des,i}(t)$  according to the spacing policy can be expressed as

$$s_{des,i}(t) = L_{i-1} + A + Tv_i(t) + Gv_i^2(t) \quad (19)$$

where  $A$  is the standstill distance and  $T = 0.0019$  and  $G = 0.0448$  are coefficients identified by the authors through offline constrained optimization. A sliding mode controller is implemented to find the follower acceleration enforcing such spacing policy. The car-following dynamics in (1) becomes

$$f_{a,i}(s_i(t), v_i(t), v_{i-1}(t)) = \frac{\lambda}{T + 2Gv_i(t)}(s_i(t) - s_{des,i}(t)) + \frac{1}{T + 2Gv_i(t)}(v_{i-1}(t) - v_i(t)) \quad (20)$$

where  $\lambda$  is a controller gain defining the sliding surface dynamics  $\dot{\epsilon} = -\lambda\epsilon$ . The sliding variable  $\epsilon$  is expressed through deviation of space headway away from desired spacing  $\epsilon = s_i(t) - s_{des,i}(t)$ . This essentially implements a VTG policy and will be referred to as "VTG SMC".

For the proposed approach, the penalty variables are prescribed as  $\rho_s = 0.1$ ,  $\rho_v = 2.0$ ,  $\rho_u = 1.0$  and  $\gamma = 0.95$ .

### 7.1 Ring Road Scenario

The first traffic simulation environment is a ring road of length  $L_{ring} = 274$  m; where  $N = 10$  homogeneous vehicles are placed uniformly and initially travelling at an equilibrium flow of  $v_{eq} = 20$  m/s. This is done through a calibrated minimum time gap of  $\tau^* = 0.96770$  s.

$$L_{ring} = Ns_{eq} = N(L_{veh} + s_0 + \tau^*v_{eq}) \quad (21)$$

However, to establish equilibrium flow at 20 m/s for IDM, a length of 348 m was needed for the ring road; where the equilibrium space headway of IDM vehicles is given as

$$s_{eq}^{IDM} = \frac{s_0 + \tau_{IDM}v_{eq}}{\sqrt{1 - \left(\frac{v_{eq}}{v_0}\right)^\delta}} \quad (22)$$

where  $\delta$  is a model parameter.

Three perturbations are introduced for Vehicle 1 in this scenario — deceleration to 15 m/s at  $t = 30$  s, then acceleration back to 20 m/s at  $t = 340$  s and, finally, sudden braking of  $2\text{m/s}^2$  at  $t = 420$  s. The resulting velocity trajectories and oblique time-space plots are shown in Figure 7. First, the string instability of the CTG ACC model is excited during the second perturbation. This induces shock-waves seen in the oblique trajectories of CTG ACC vehicles in Figure 7; which eventually cause the vehicles to stop resulting in phantom jams or stop-and-go waves. In contrast, the VTG ACC and VTG SMC schemes show string stable trajectories and attenuate all disturbances accordingly. Interestingly, the proposed spacing policy VTG ACC is better at achieving a balance in space gaps than the VTG SMC policy, as illustrated in Figure 8. The balanced space gaps of the perturbing vehicle "V1" and its following vehicle "V2" demonstrates a potential of better road space utilization while dissipating disturbances. Regarding human driving, all three perturbations are attenuated; however, at a slower rate than the variable spacing schemes. Generally, the second and third perturbations show more aggressive effects.

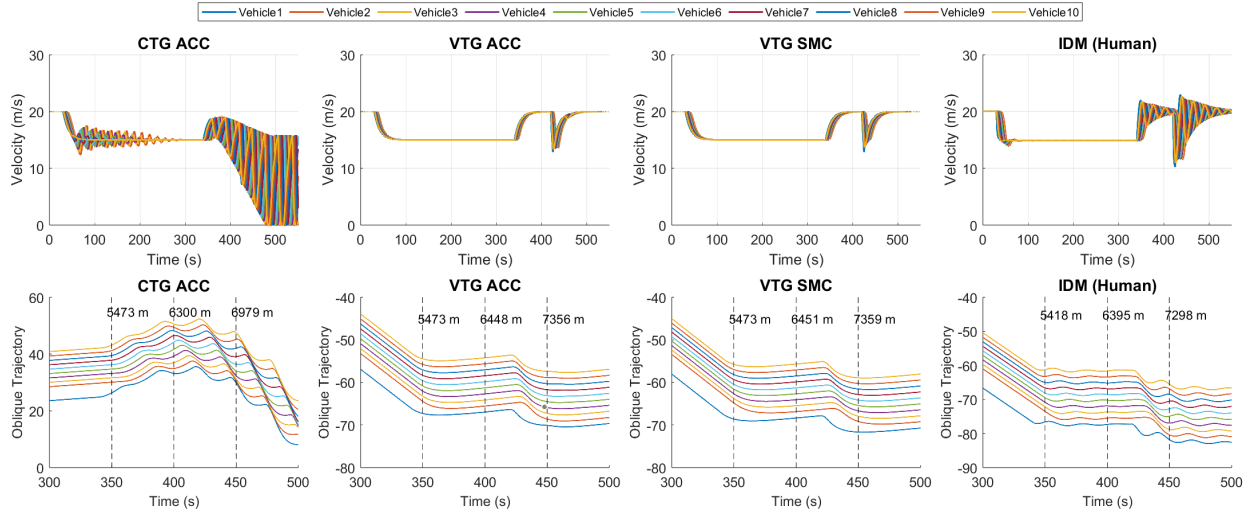


Figure 7: Velocity profiles and oblique trajectories of 10 vehicles in a ring road scenario.

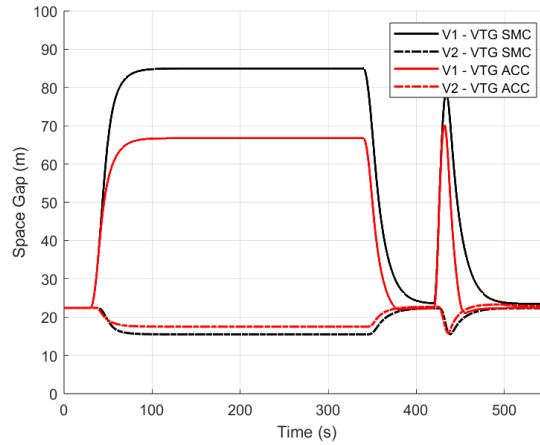


Figure 8: Spacing trajectories of 2 vehicles following the variable spacing policies of VTG SMC and VTG ACC.

The ring road simulation scenario is repeated to investigate the performance of the proposed algorithm and the cooperative mixed  $\mathcal{H}_2/\mathcal{H}_\infty$  algorithm introduced by [31]. Here, we consider homogeneous platoons of ACC-enabled vehicles for implementation of the centralized controller by [31] for comparison. This test is carried out for a platoon of  $N = 5$  vehicles in a ring road of length  $L_{\text{ring}} = 137$  m as well as the calibrated minimum time gap of  $\tau^* = 0.96770$  s. Initial perturbations in the vehicles velocities are introduced as well as a sharp deceleration of  $-3 \text{ m/s}^2$  lasting 3 s for one random vehicle — 'Vehicle 3' in Figure 9.

As illustrated in Figure 9, both schemes are able to dissipate perturbations as they are string stable by design. However, the centralized ACC algorithm shows lower changes in space and time headway relative to the proposed VTG ACC algorithm. The reason is that the former scheme assumes a centralized cooperative structure; therefore, has global information about all platoon vehicles. In contrast, our proposed control scheme is completely decentralized via predecessor-follower topology and only needs sensor measurements of spacing and lead velocity; thus, it is more computationally efficient with comparable performance. Interestingly, with the heightened interest in connected vehicles, our proposed scheme can be extended for connected vehicles which is left for future research.

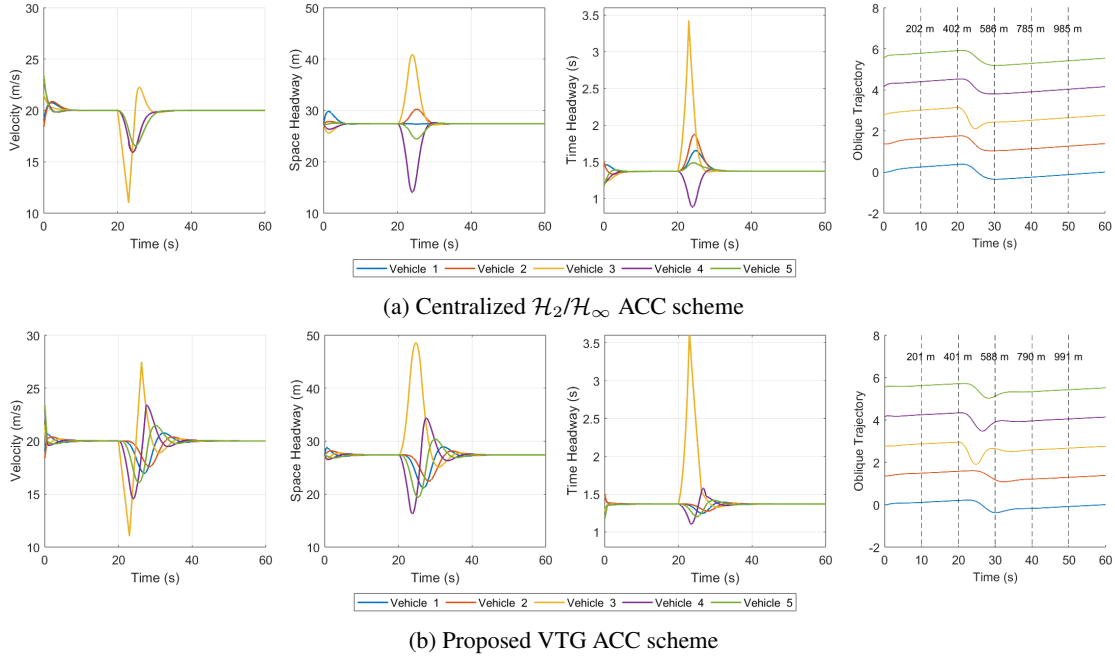


Figure 9: Simulated trajectories of a platoon of 5 vehicles along a ring road.

## 7.2 Highway Merging Scenario

In this scenario, a single-lane highway of length 1 km has an on-ramp merging at position 600 m. The maximum flow rate of vehicles at the mainline is 2000 veh/h while the on-ramp creates a demand of 100 veh/hr. The vehicles' arrival on both the highway and the on-ramp are modelled as independent Poisson processes with the corresponding flow rate. The vehicles on the mainline have a steady-state speed of 30 m/s. The aggressive joining of vehicles from the on-ramp to the mainline may cause shock-waves downgrading the system performance. The default lane change model of SUMO is used in this simulation scenario.

A mixed traffic flow is created by varying the penetration rate,  $p$ , of the ACC-equipped vehicles; i.e. controlled by either CTG ACC, VTG ACC or VTG SMC. The calibrated CTG ACC algorithm represents the commercially-available ACC systems and the calibrated IDM algorithm represents manually driven vehicles. Here, the performance of the traffic system is evaluated by average outflow from the network versus penetration rates of  $p = [0, 10\%, 25\%, 50\%, 75\%, 100\%]$ ; which is summarized by Figure 10. These are obtained by averaging 10 600-second runs. The proposed VTG ACC scheme for  $\rho_u = 0.75$  yields an improved traffic outflow in comparison to both the CTG ACC and the VTG SMC algorithms. Interestingly, the VTG SMC achieves lower outflow due to larger space gaps required by the adopted quadratic spacing policy for speeds higher than around 21 m/s; as shown in Figure 11. Thus, the improvement in the traffic outflow exhibited by the proposed algorithm can be attributed to (a) dissipating perturbations created by the merging bottleneck and (b) adhering to a constant minimum time gap policy during stable car-following conditions which shows better road space utilization and traffic efficiency.

On the other hand, for the case of  $\rho_u = 1.0$ , the VTG ACC algorithm is more conservative with respect to string stability enforcement and minimizing the manipulated time-gap component  $u_i(t)$  compared to the case of  $\rho_u = 0.75$ . This can be further observed in Figure 12 where the time-space diagrams are shown for  $p = 100\%$  and fully manually driven traffic flow. The VTG ACC algorithm with  $\rho_u = 1.0$  shows less perturbations and shock-waves formed compared to  $\rho_u = 0.75$ . However, the traffic volume yielded after the on-ramp merging bottleneck is higher for  $\rho_u = 0.75$  due to a

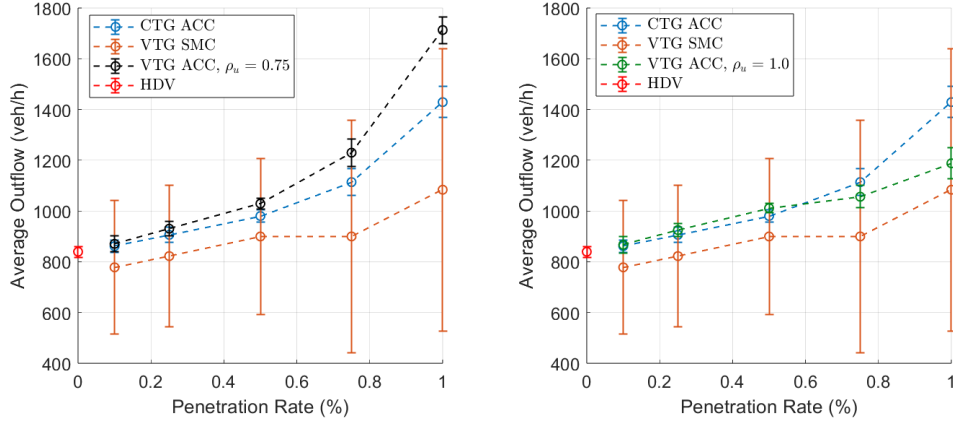


Figure 10: Average outflow from the highway merge network for different penetration rates of ACC-equipped vehicles.

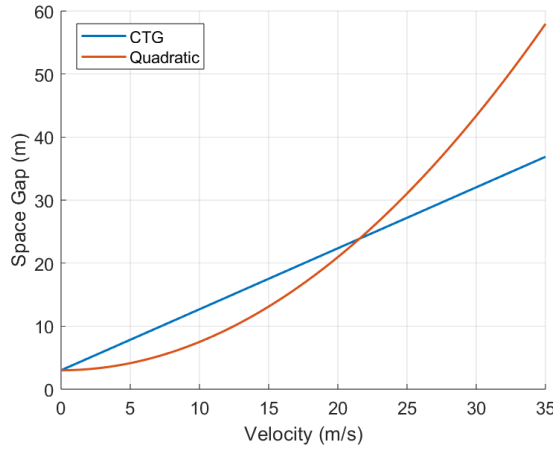


Figure 11: Constant time-gap (CTG) and quadratic spacing policies during stable car-following conditions.

more relaxed VTG policy. Additionally, the performance indicators for safety and energy consumption are computed for each vehicle in the network and the ratio of improvement with respect to the calibrated CTG ACC averaged over all vehicles is computed. As illustrated in Table 1, the maximum improvement in minimum TTC per vehicle is observed for the case of  $\rho_u = 1.0$  as string stability is conservatively enforced; whereas more improvement is seen in tractive energy consumption for  $\rho_u = 0.75$ . This can be attributed to the more relaxed VTG policy which gives rise to a more smooth accommodation of the flow of merging vehicles with relaxed time headways. Hence, an adjustment of the penalty variable  $\rho_u$  may result in different behaviors since it allows various degrees of relaxation of the CTG policy and string stability enforcement.

Table 1: Average ratio of improvement of performance indicators for the proposed VTG ACC scheme with respect to the calibrated CTG ACC scheme.

Penetration Rate	VTG ACC, $\rho_u = 0.75$		VTG ACC, $\rho_u = 1.0$	
	minimum TTC	$E_c$	minimum TTC	$E_c$
10%	0.021	0.025	0.10	0.014
25%	0.044	0.42	0.25	-0.013
50%	0.057	1.61	0.42	-0.10
75%	0.094	5.33	1.05	-0.0069
100%	0.26	2.97	2.59	-0.13

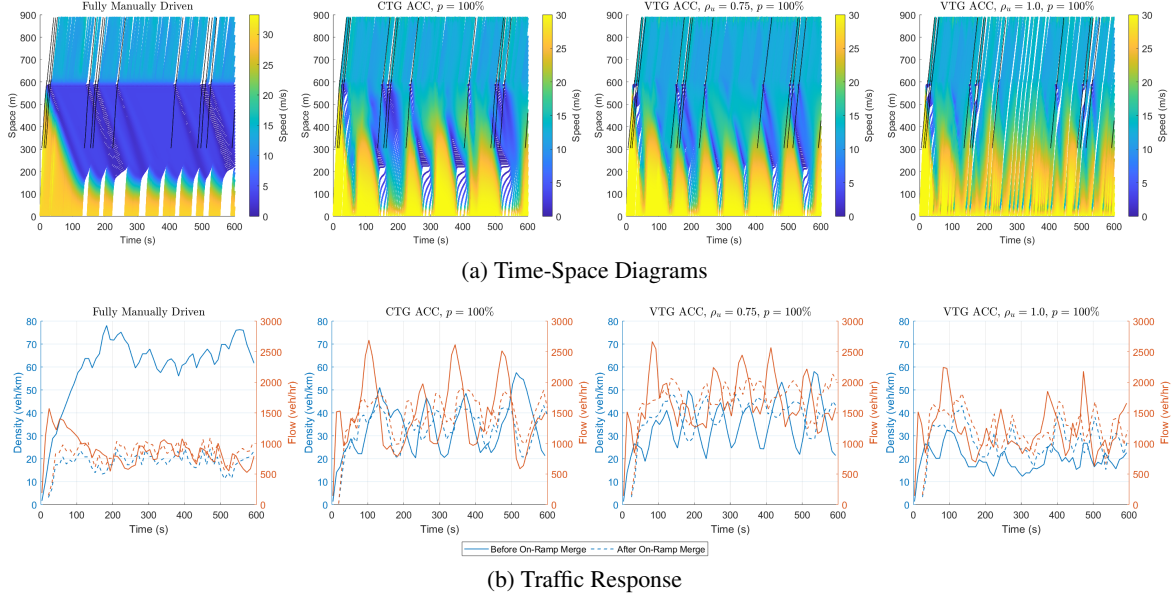


Figure 12: Time-space diagrams and traffic response in a highway merging network using the calibrated CTG ACC and the proposed VTG ACC.

## 8 Conclusion

In this article, a variable time gap strategy is designed to guarantee string stability in the strict sense for vehicle platoons. The control architecture is modular; where a constant time gap component  $\tau^*$  and a variable time gap component  $u(t)$  is designed as the control policy for disturbance attenuation. Strict string stability is guaranteed through nonlinear  $\mathcal{H}_\infty$  control to dissipate perturbations from the leading vehicle to the prescribed penalty variables; space headway and ego vehicle's velocity. The string stability problem is decoupled from equilibrium flow dictated by  $\tau^*$ ; which may define driver comfort settings or a minimum time gap value for traffic efficiency. The performance of the proposed scheme is validated through numerical simulations compared to calibrated models representing commercially available ACC systems and manually driven vehicles; available in the OpenACC dataset, as well as variable spacing policies from the literature. Also, traffic simulations are carried out to demonstrate the efficacy of each model in both a ring road scenario and a highway merging scenario. Notably, under a penetration rate of 10%, the proposed VTG ACC policy improved traffic outflow by 1.05% on average compared to the CTG ACC policy (representing commercially available ACC systems); as well as relieving safety and energy efficiency concerns with an improvement of 2.1% and 2.5% respectively.

## Acknowledgments

The authors would like to thank Dr. Yifan Zhang for the insightful discussions on car-following models.

## References

- [1] SAE, "Society of Automotive Engineers J3016: Taxonomy and definitions for terms related to driving automation systems for on-road motor vehicles," 2021.
- [2] M. Shang and R. E. Stern, "Impacts of commercially available adaptive cruise control vehicles on highway stability and throughput," *Transportation Research Part C: Emerging Technologies*, vol. 122, p. 102897, 1 2021.
- [3] C. Wu, Z. Xu, Y. Liu, C. Fu, K. Li, and M. Hu, "Spacing policies for adaptive cruise control: A survey," *IEEE Access*, vol. 8, pp. 50149–50162, 2020.
- [4] I. A. Ntousakis, I. K. Nikolos, and M. Papageorgiou, "On microscopic modelling of adaptive cruise control systems," *Transportation Research Procedia*, vol. 6, pp. 111–127, 2015.

- [5] Y. Bian, Y. Zheng, S. E. Li, Z. Wang, Q. Xu, J. Wang, and K. Li, "Reducing time headway for platoons of connected vehicles via multiple-predecessor following," *IEEE Conference on Intelligent Transportation Systems, Proceedings, ITSC*, vol. 2018-November, pp. 1240–1245, 12 2018.
- [6] M. Makridis, K. Mattas, A. Anesiadou, and B. Ciuffo, "Openacc. an open database of car-following experiments to study the properties of commercial acc systems," *Transportation Research Part C: Emerging Technologies*, vol. 125, p. 103047, 2021.
- [7] B. Ciuffo, K. Mattas, M. Makridis, G. Albano, A. Anesiadou, Y. He, S. Josvai, D. Komnos, M. Pataki, S. Vass, and Z. Szalay, "Requiem on the positive effects of commercial adaptive cruise control on motorway traffic and recommendations for future automated driving systems," *Transportation Research Part C: Emerging Technologies*, vol. 130, p. 103305, 9 2021.
- [8] V. Milanés and S. E. Shladover, "Modeling cooperative and autonomous adaptive cruise control dynamic responses using experimental data," *Transportation Research Part C: Emerging Technologies*, vol. 48, pp. 285–300, 2014.
- [9] G. Gunter, D. Gloudemans, R. E. Stern, S. McQuade, R. Bhadani, M. Bunting, M. L. D. Monache, R. Lysecky, B. Seibold, J. Sprinkle, B. Piccoli, and D. B. Work, "Are commercially implemented adaptive cruise control systems string stable?," *IEEE Transactions on Intelligent Transportation Systems*, vol. 22, pp. 6992–7003, 2021.
- [10] T. W. Lin, S. L. Hwang, and P. A. Green, "Effects of time-gap settings of adaptive cruise control (acc) on driving performance and subjective acceptance in a bus driving simulator," *Safety Science*, vol. 47, pp. 620–625, 5 2009.
- [11] J. Wang and R. Rajamani, "Adaptive cruise control system design and its impact on highway traffic flow," *Proceedings of the American Control Conference*, vol. 5, pp. 3690–3695, 2002.
- [12] J. Zhou and H. Peng, "Range policy of adaptive cruise control for improved flow stability and string stability," *Conference Proceeding - IEEE International Conference on Networking, Sensing and Control*, vol. 1, pp. 595–600, 2004.
- [13] D. Swaroop and K. R. Rajagopal, "Intelligent cruise control systems and traffic flow behavior," *ASME International Mechanical Engineering Congress and Exposition, Proceedings (IMECE)*, vol. 1999-J, pp. 373–380, 1999.
- [14] S. Feng, Y. Zhang, S. E. Li, Z. Cao, H. X. Liu, and L. Li, "String stability for vehicular platoon control: Definitions and analysis methods," *Annual Reviews in Control*, vol. 47, pp. 81–97, 1 2019.
- [15] M. Montanino and V. Punzo, "On string stability of a mixed and heterogeneous traffic flow: A unifying modelling framework," *Transportation Research Part B: Methodological*, vol. 144, pp. 133–154, 2 2021.
- [16] A. Kesting, M. Treiber, M. Schönhof, and D. Helbing, "Adaptive cruise control design for active congestion avoidance," *Transportation Research Part C: Emerging Technologies*, vol. 16, pp. 668–683, 2008.
- [17] M. Wang, W. Daamen, S. P. Hoogendoorn, and B. van Arem, "Rolling horizon control framework for driver assistance systems. part i: Mathematical formulation and non-cooperative systems," *Transportation Research Part C: Emerging Technologies*, vol. 40, pp. 271–289, 2014.
- [18] A. Spiliopoulou, D. Manolis, F. Vandorou, and M. Papageorgiou, "Adaptive cruise control operation for improved motorway traffic flow," *Transportation Research Record*, vol. 2672, pp. 24–35, 2018.
- [19] J. Chen, Y. Zhou, and H. Liang, "Effects of acc and cacc vehicles on traffic flow based on an improved variable time headway spacing strategy," *IET Intelligent Transport Systems*, vol. 13, pp. 1365–1373, 2019.
- [20] J. Wang and R. Rajamani, "Should adaptive cruise-control systems be designed to maintain a constant time gap between vehicles?," *IEEE Transactions on Vehicular Technology*, vol. 53, pp. 1480–1490, 2004.
- [21] D. Yanakiev and L. Kanellakopoulos, "Nonlinear spacing policies for automated heavy-duty vehicles," *IEEE Transactions on Vehicular Technology*, vol. 47, pp. 1365–1377, 1998.
- [22] J. Dong, J. Wang, L. Chen, Z. Gao, and D. Luo, "Effect of adaptive cruise control on mixed traffic flow: A comparison of constant time gap policy with variable time gap policy," *Journal of Advanced Transportation*, vol. 2021, 2021.
- [23] N. Bekiaris-Liberis and A. I. Delis, "Pde-based feedback control of freeway traffic flow via time-gap manipulation of acc-equipped vehicles," *IEEE Transactions on Control Systems Technology*, vol. 29, pp. 461–469, 2021.
- [24] M. Treiber and A. Kesting, *Traffic Flow Dynamics*. 2013.
- [25] R. L. Kosut, "Uncertainty model unfalsification: A system identification paradigm compatible with robust control design," *Proceedings of the IEEE Conference on Decision and Control*, pp. 3492–3497, 1995.
- [26] K. V. Heusden, A. Karimi, and D. Bonvin, "Data-driven estimation of the infinity norm of a dynamical system," *Proceedings of the IEEE Conference on Decision and Control*, pp. 4889–4894, 2007.

- [27] M.-A. Massoumnia and R. L. Kosut, "A family of norms for system identification problems," *IEEE Transactions on Automatic Control*, vol. 39, pp. 1027–1031, 1994.
- [28] J. Huang and C. F. Lin, "Numerical approach to computing nonlinear  $\mathcal{H}_\infty$  control laws," *Journal of Guidance, Control, and Dynamics*, vol. 18, pp. 989–994, 1995.
- [29] T. Apostolakis and K. Ampountolas, "Physics-inspired neural networks for parameter learning of adaptive cruise control systems," 9 2023.
- [30] Y. He, M. Montanino, K. Mattas, V. Punzo, and B. Ciuffo, "Physics-augmented models to simulate commercial adaptive cruise control (acc) systems," *Transportation Research Part C: Emerging Technologies*, vol. 139, p. 103692, 2022.
- [31] S. S. Mousavi, S. Bahrami, and A. Kouvelas, "A mixed  $\mathcal{H}_2/\mathcal{H}_\infty$  controller design for a platoon with multiple human-driven and connected and automated vehicles," *2023 European Control Conference, ECC 2023*, 2023.